

Fundamental-mode fiber-to-fiber coupling at high-power

Mats Blomqvist*^a, Magnus Pålsson^a, Ola Blomster^a, Göran Manneberg^b

^aOptoskand AB, Krokslätts Fabriker 27, SE-431 37 Mölndal, Sweden;

^bBiomedical and X-Ray Physics, AlbaNova University Center/Royal Institute of Technology, SE-106 91 Stockholm, Sweden

ABSTRACT

Fiber-to-fiber coupling between two different fibers is a state of the art technology. Products are available on the market where multimode fibers can be coupled with very low power loss, at very high powers (multi-kilowatt). We have, however, always been forced to accept a certain loss in beam quality, manifesting as an increase in the Beam Parameter Product (BPP). In fundamental-mode fiber-to-fiber coupling no beam quality is lost. We instead expect to have a certain power loss in the coupling.

This paper addresses the problems in free-space fundamental-mode fiber-to-fiber coupling, including theoretical estimations of expected power loss, estimated demands on the stability of the optics as well as measured values on a fundamental mode fiber-to-fiber coupler.

The theoretical calculations of the sensitivity of the coupling efficiency due to radial misalignment and defocus (longitudinal displacement) have been confirmed experimentally. Experimental results at 100 W laser power include 88% coupling efficiency using a large mode area fiber with mode-field diameter (MFD) of 18 μm and 75 % coupling efficiency using a single-mode fiber with MFD of 6.4 μm .

Keywords: Fundamental-mode, fiber-to-fiber coupling, high-power, Fresnel transformation, beam parameters

1. INTRODUCTION

Today high-power lasers are frequently used in various industrial applications, such as welding and cutting. In order to protect for example a feeding fiber of a high-power fiber laser, multimode fiber-to-fiber couplers are commonly used. Using multimode fiber-to-fiber couplers part of the Beam Parameter Product (BPP) is sacrificed and the power losses are minimized. With the development of fundamental-mode lasers in the multi-kilowatt range, there is an increasing interest to extend the free-space fiber-to-fiber couplers to handle such lasers. In fundamental-mode fiber-to-fiber coupling beam quality has to be maintained. Thus, instead of mainly having beam quality losses in multimode fiber-to-fiber coupling, fundamental-mode fiber-to-fiber coupling will exhibit power losses.

This paper addresses the problems in fundamental-mode fiber-to-fiber coupling, including theoretical estimations of expected power losses, estimated demands on the stability of the coupling optics as well as measured values on a fundamental mode fiber-to-fiber coupler.

1.1 Scope of the Paper

Theoretical and experimental results will be presented for two different configurations. The starting point in both configurations is a single-mode fiber with mode-field diameter (MFD) of $6.4 \pm 0.5 \mu\text{m}$ and numerical aperture $\text{NA} = 0.14 \pm 0.01$. The optical power ($\lambda = 1090 \pm 5 \text{ nm}$) exiting this fiber is collimated using a diameter 10 mm, $f = 24 \text{ mm}$ quartz doublet (QD) lens. In the first fully symmetric configuration, the collimated beam is focused with an identical $f/24$ QD lens into a single-mode fiber of the same kind as the feeding fiber. In the second configuration, the collimated beam is focused with a diameter 25 mm, $f = 50 \text{ mm}$ quartz triplet (QT) into a large mode area (LMA) fiber with $\text{MFD} = 18 \pm 1 \mu\text{m}$ and $\text{NA} = 0.06 \pm 0.01$.

* mats.blomqvist@optoskand.se; phone +46 31 706 27 82; fax +46 31 706 27 78; www.optoskand.se

2. THEORETICAL

2.1 Extent of the Theoretical Study

When coupling light from one fiber to another, the fraction of light power coupled is called the coupling efficiency. In multimode fibers this can be quite accurately predicted with rather crude methods based on geometrical optics and the concept of numerical aperture. For single mode fibers the situation becomes somewhat more complex and the coupling efficiency is described by overlap integrals of the field at the in-coupling surface and the possible field of the mode in the receiving fiber. Both fields are then assumed to be normalized. In such integrals the phase distribution often plays a much more important role than actual overlap of the envelopes.

In this theoretical part, the aim is to determine the sensitivity of the coupling efficiency to misalignments of different types, such as radial misalignment, defocusing and tilt. The theoretical study is limited to the case of optics with negligible aberrations and negligible diffraction in the lenses. The starting point is the image of the out-coupled field found in the Gaussian image plane of the system(s) used for collimation and focusing of the beam. This field is then Fresnel transformed to the surface where the actual fiber is found, where the overlap integral is calculated.

2.2 Choice of Out-coupled Field

For the theoretical calculations, the choice of the out-coupled field has to be considered. If the wave equation is solved for the cylindrical geometry of a fiber the mathematical solution is a combination of Bessel functions of first and forth kind chosen so that the field, but not its derivatives, is continuous at the border between core and cladding. For single mode operation of a fiber the only mode is described by the zeroth order Bessel functions. This is an awkward function to work with mainly because of the discontinuities, which makes the transition between near field and far field mathematically cumbersome. In order to describe the field from a fiber a Gaussian function is often used as an approximation. This has several advantages:

- The mathematical apparatus described in many textbooks for Gaussian beams can be used directly.
- Both near field and far field are described by the same function as a consequence of the fact that a Gaussian function is its own Fourier transform.
- The behavior of Gaussian beams is widely and intuitively known.

The main drawback is that the Gaussian approximation is not very accurate. Errors made are in the 10% order of magnitude especially for large values of the radius, r , where the Gaussian function drops far too rapidly. An alternative approximation is the hyperbolic secant function (sech or sechyp), which is the same as the inverse cosine hyperbolic function. This function approximates the field much better than the Gaussian and errors are in the single percent range. It also has the property of being its own Fourier transform. The only drawback of the hyperbolic secant function is that the Gaussian apparatus does not work. In this theoretical study the hyperbolic secant function will be used to describe the out-coupled field.

2.3 Field around the Image Plane

The field of an optical beam propagating in air or any other medium can be found by the Fresnel-Kirchhoff integral transform between planes 1 and 2, separated L , given by

$$E(x_2, x_1) = \text{const} \iint_{\text{field}} \exp i \left(\frac{2\pi}{\lambda} \sqrt{L^2 + (x_2 - x_1)^2 + (y_2 - y_1)^2} \right) dx dy, \quad (1)$$

where λ is the wavelength. This integral is the starting point for the Fresnel and Fraunhofer approximations used in wave theory. The reason for making approximations (e.g. series expansions of the root expression) is the search for analytical solutions, which is not really relevant in this study, so the root expression in the exponential will be kept. This implies that the amplitude and phase distributions around the image plane to see the effect of longitudinal defocus can be calculated. In principle, this can always be performed meaning that all optical design programs could use this method. The reason it seldom is performed is that accurate calculation requires very dense sampling. Calculating the field given by a field 1 cm² in cross section would require 10⁸ contribution patches for each field point in plane 2. This means 10¹⁶ calculations, which is of course prohibitive. In this study the starting point is a much smaller field, which keeps the

number of calculations reasonable. The validity of the numerical integral has been checked by looking for Cartesian artifacts in the phase maps of the field around a defocused beam waist.

2.4 Receiving Fiber and Imaging

The receiving fiber geometry is described by its defocus (longitudinal displacement), its radial displacement (misalignment) and its tilt (angular misalignment). The mode field diameter is defined as $2\omega_1$ in

$$A = A_0 \operatorname{sech}\left(\frac{2r}{\omega_1}\right), \quad (2)$$

The numerical aperture is given for both possible fibers.

As mentioned in 2.1 the imaging is assumed to be without both aberrations and diffraction. The condition for this is that aberrations give smaller effects than diffraction and diffraction in the lenses is negligible. For the two lens combinations the entrance pupil radius is double the modal radius at the entrance pupil which means lens diffraction can be neglected within errors of single percents.

Treating the imaging with geometric optics can of course be questioned, but for both Gaussian and hyperbolic secant beams the radius of the beam (if treated rigorously) is given by the geometrical magnification as long as no lens elements are placed near or within the Rayleigh range, which is clearly the case in this application.

2.5 Calculation of the Coupling Efficiency

The coupling efficiency is calculated with the help of overlap integrals between defocused field, E , and the radially translated receiving fiber mode, A :

$$C = \frac{\int E(x, y, \Delta z) dx dy \cdot \int A^*(x, y, \Delta r) dx dy}{\sqrt{\int EE^* dx dy \cdot \int AA^* dx dy}}. \quad (3)$$

The coupling efficiency is the presented as a function of radial misalignment and defocus.

2.6 Effects of Tilting

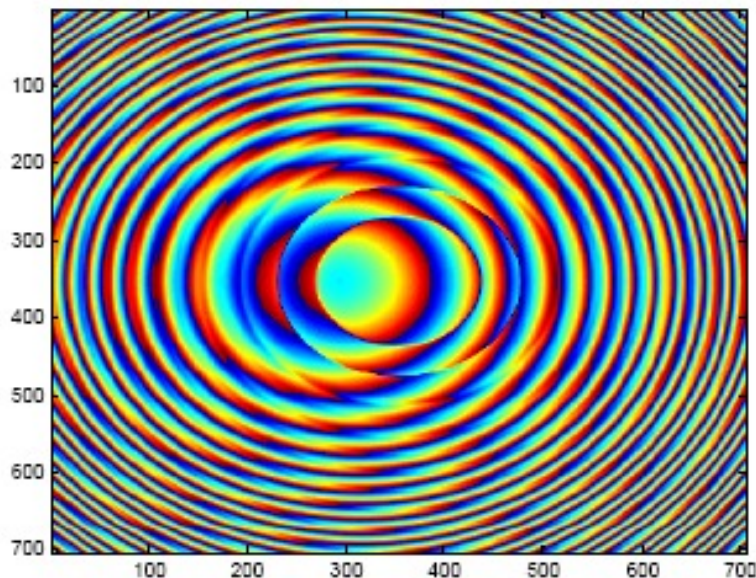


Fig. 1. The figure shows the phase map at the entrance of a tilted fiber. The discontinuities that can be seen correspond to phase jumps of 2π . In this specific plot the field is at 50 mrad tilt and 120 μm defocus.

The dominating effect of tilting the fiber is the phase error. Fig. 1. shows the phase map at the entrance of a tilted fiber, where the discontinuities correspond to phase jumps of 2π . In this context it should be pointed out that tilt of the receiving fiber is roughly equivalent to a twice as large error in surface angle, since

$$\text{Real cut angle} = \frac{\text{tilt angle}}{n_{\text{core}} - 1}. \quad (4)$$

Simulations of the effect of tilting indicate reduction in the coupling efficiency below 3 % for tilting angles up to 20 mrad, thus it is possible to neglect this error.

3. EXPERIMENTAL

The purpose of the experiments was to validate the results from the theoretical simulations, and to examine the sensitivity of the coupling efficiency due to the various misalignments. Also, power transmission and beam profile was measured.

3.1 Experimental Setup

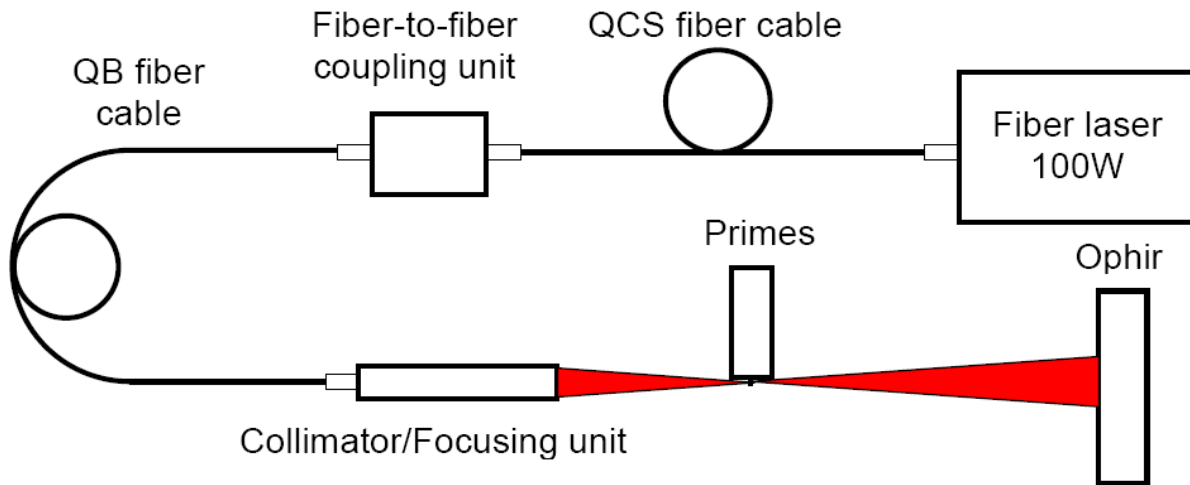


Fig. 2. The figure shows a schematic description of the experimental setup.

A schematic description of the experimental setup is shown in Fig. 2. The high power laser used in this experiment was a fiber laser with 100 W maximum output power at approximately $\lambda = 1090$ nm. The output from the collimated QCS fiber (MFD = 6.4 ± 0.5 μm , NA = 0.14 ± 0.01) was connected via a modified *Optoskand* fiber-to-fiber coupling unit (FFC). The focusing lens of the FFC is interchangeable ($\text{Ø}10$ mm, $f = 24$ mm quartz doublet or $\text{Ø}25$ mm, $f = 50$ mm quartz triplet). Two different special *Optoskand* QB fibers were used on the output side of the FFC; one using the same fiber as in the QCS fiber cable and one fiber using a LMA fiber with MFD = 18 ± 1 μm and NA = 0.06 ± 0.01 . The fibers were adjusted with the standard screws on the FFC, having a resolution of 35 μm /turn in the xy-directions and 0.5 mm/turn in the z-direction. To measure the beam parameters a *Primes FocusMonitor* was used after an $f60/f205$ mm collimator/focusing optics. The power was measured with an *Ophir* head.

4. RESULTS

In this section theoretical and experimental results will be presented. The theoretical simulations were performed using *MATLAB* on a personal computer.

4.1 Calculated Coupling Efficiency

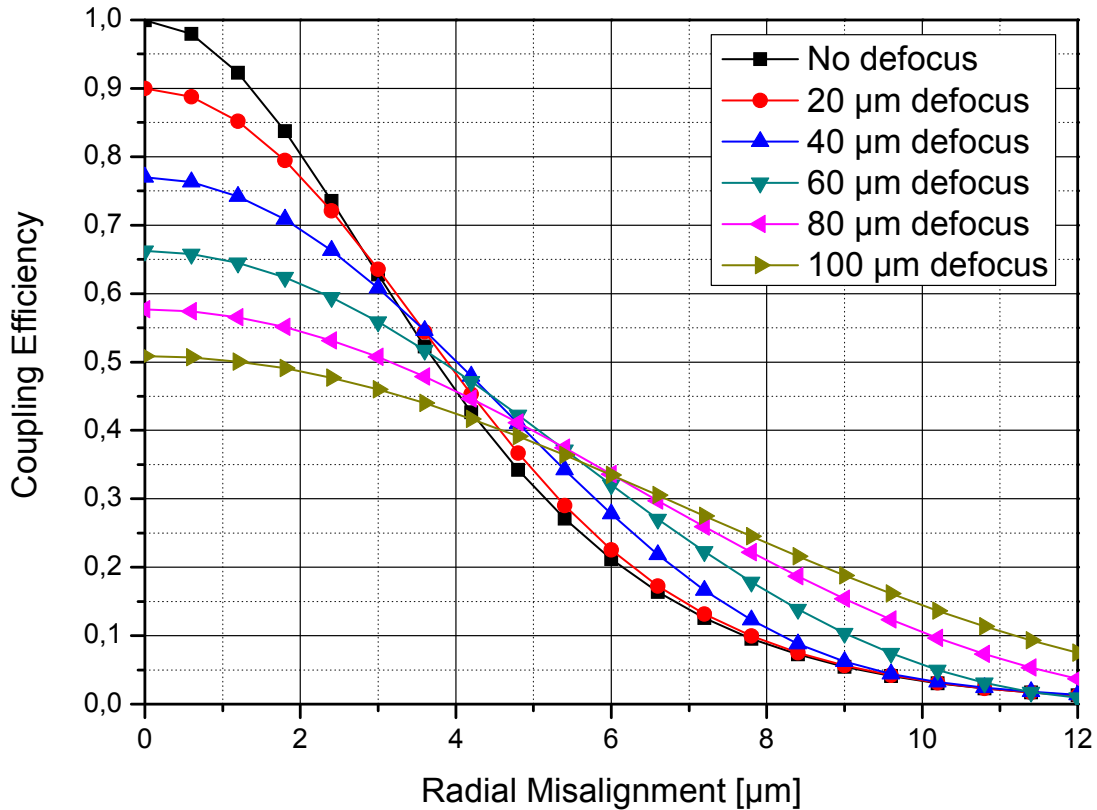


Fig. 3. Shows the coupling efficiency in the symmetric case coupling into a single-mode fiber with $\omega_1 = 3.2 \mu\text{m}$ using an $f = 24 \text{ mm}$ lens. The different curves describe defocused situations.

In Fig. 3. the theoretical calculations for the symmetric case with coupling into a single-mode fiber with $\omega_1 = 3.2 \mu\text{m}$ using an $f = 24 \text{ mm}$ lens is presented. The curve starts at coupling efficiency = 1.0 for perfect focus and no misalignment. This is of course a result from not including residual Fresnel losses and other imperfections. As can be expected the focused case (black curve/square symbols) is most sensitive to radial misalignment, and it drops to 50% already at $3.7 \mu\text{m}$ misalignment. If we are defocused $100 \mu\text{m}$ (dark yellow curve/right triangle symbols) the efficiency is much more insensitive to misalignment. In the defocused case the drop in efficiency is due the lack of phase compatibility and in the misaligned it is because of non-overlapping envelopes.

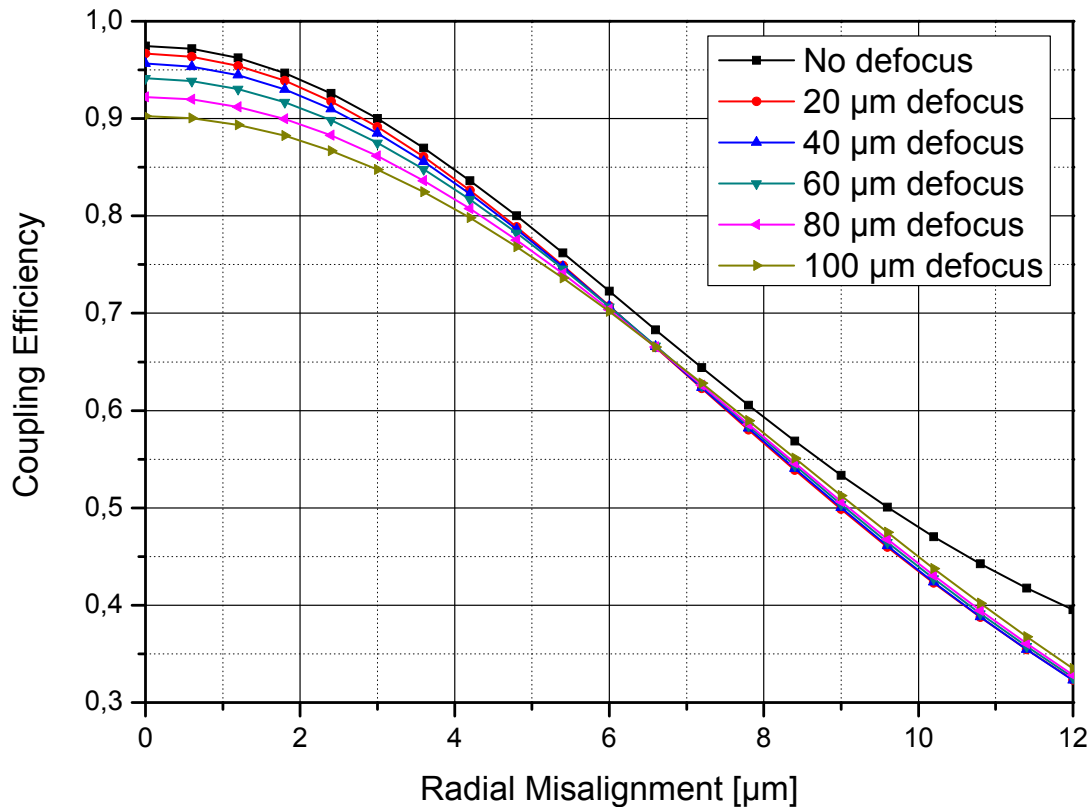


Fig. 4. Shows the coupling efficiency in the asymmetric case coupling into a single-mode fiber with $\omega_1 = 9 \mu\text{m}$ using an $f = 50 \text{ mm}$ lens. The different curves describe defocused situations.

The asymmetric case coupling into a large mode area fiber with $\omega_1 = 9 \mu\text{m}$ using an $f = 50 \text{ mm}$ lens is presented in Fig. 4. The curve for perfect focus and no misalignment starts close to coupling efficiency = 1.0. Mismatch in numerical aperture is the cause for not being exactly 1.0. Misalignment tolerance is almost $10 \mu\text{m}$ for 50% coupling efficiency and defocus tolerance is very good because the mode is smaller than the fiber but still has good Rayleigh range.

4.2 Measured Coupling Efficiency

From the theoretical simulations the symmetric situation coupling into a single-mode fiber is the most sensitive case. This was confirmed in the experimental work, where the radial misalignment tolerance is very small. The resolution of the two xy-screws is $35 \mu\text{m}/\text{turn}$, which implies only 1/10 of a turn for the coupling efficiency to drop down to around 50%. Also finding the optimal defocus position is challenging, partly because of the lower resolution of the z-alignment screw, and partly because of the hysteresis of the alignment screw.

Due to the relatively large expected losses when misaligning, the measurements were performed at approximately 10 W laser power output.

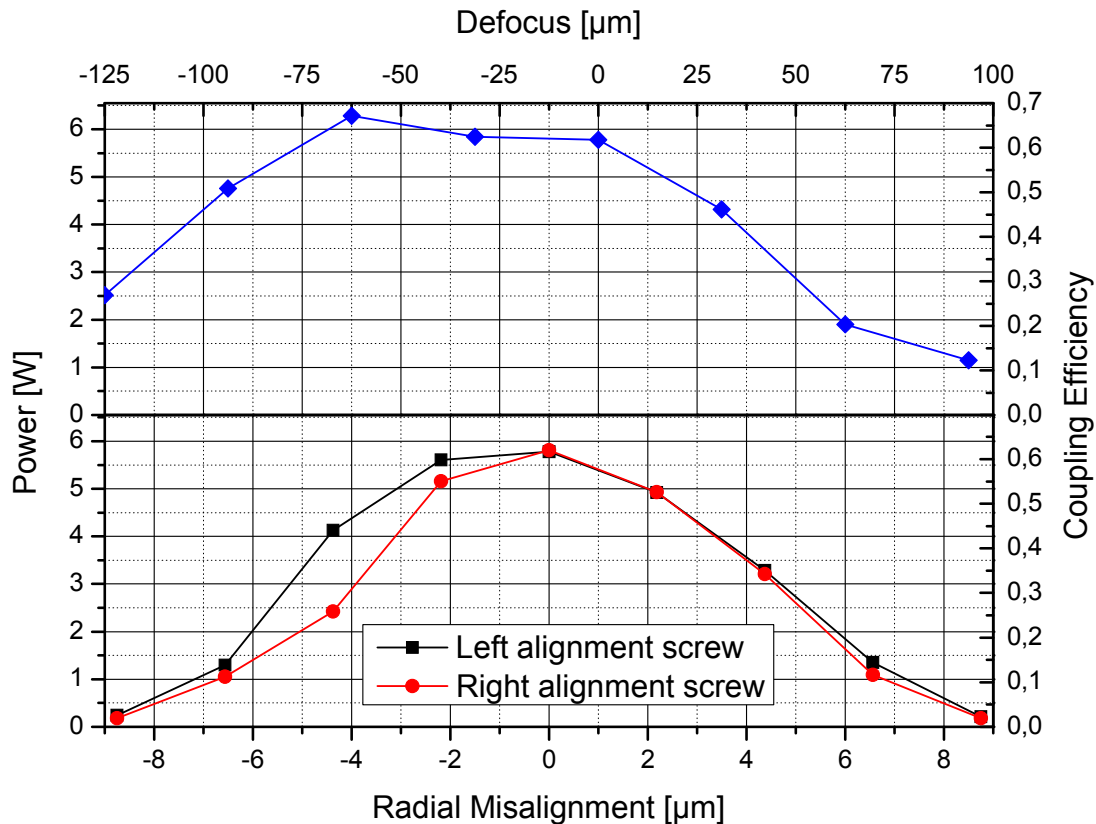


Fig. 5. The coupling efficiency as a function of radial misalignment and defocusing for the symmetric case coupling into a single-mode fiber with $\omega_1 = 3.2 \mu\text{m}$ using an $f = 24 \text{ mm}$ lens.

The lower part of Fig. 5. shows the coupling efficiency as a function of radial misalignment, where the defocus has been optimized. As can be seen the coupling efficiency only reaches about 62%, which implies a certain degree of defocus. The radial misalignment coupling efficiency follows the simulations to large extent, where the power drops to 50% within approximately $\pm 5 \mu\text{m}$.

The upper part of Fig. 5. shows the dependency of defocus, where at each measurement point the radial misalignment has been optimized. The center flatness is an indication of the difficulty in finding the optimal position, but qualitatively the measurement agrees with the simulations.

After the misalignment measurements, the xy- and z-positions were optimized and the laser power increased. At 100 W output power, transmission through a multi-mode fiber with 100- μm core was measured to 96.2 W. At the same conditions, the transmission through the single-mode fiber was 72 W, indicating an overall coupling efficiency of 75 %. The lower coupling efficiency compared to the simulated value is attributed to alignment tolerances, losses from residual Fresnel losses and other imperfections in the lens systems, and in variations of the single-mode fiber regarding MFD and NA.

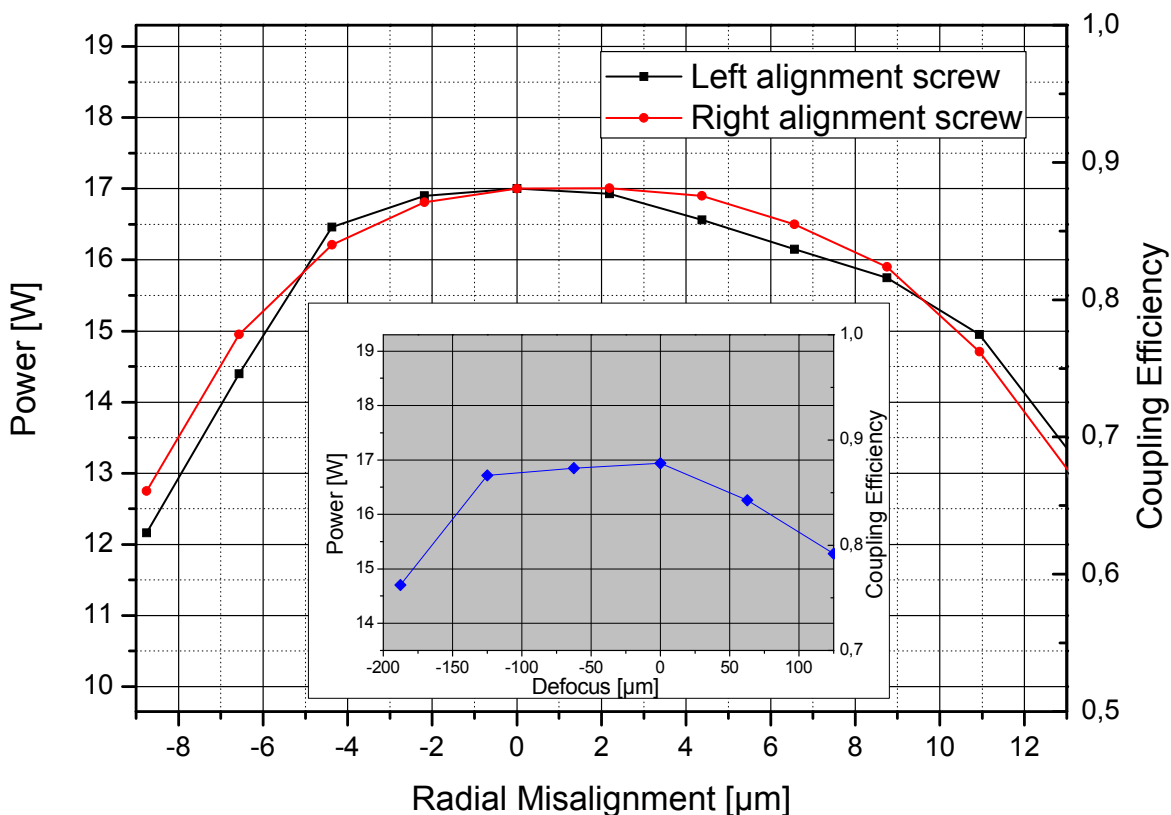


Fig. 6. The coupling efficiency as a function of radial misalignment for the asymmetric case coupling into a large mode area fiber with $\omega_1 = 9 \mu\text{m}$ using an $f = 50 \text{ mm}$ lens. The inset shows the defocus behavior, where each measurement point is radially aligned.

Fig. 6. shows the coupling efficiency for the asymmetric case with the LMA fiber and the $f = 50 \text{ mm}$ lens measured at nominally 20 W output laser power. As expected the alignment was less sensitive for this case. The maximum coupling efficiency reached above 88% and the coupling efficiency curves as a function of radial misalignment follows the theoretical calculations quite well. The inset of Fig. 6. shows the defocus behavior, where each measurement point is radially aligned. Within $\pm 100 \mu\text{m}$ defocus there is a change in coupling efficiency of around 5%, in good agreement with the theoretical simulations.

After the misalignment measurements, the xy - and z -positions were optimized and the laser power increased to 100 W output power, where the transmission through a multi-mode fiber with 100- μm core was measured to 97.1 W. At the same conditions, the transmission through the single-mode fiber was 85.1 W, indicating an overall coupling efficiency of 88 %.

4.3 Beam Parameter Measurements

The beam parameters were measured at 20 W and 50 W for the single-mode fiber with $\omega_1 = 3.2 \mu\text{m}$ and the large mode area fiber with $\omega_1 = 9 \mu\text{m}$, respectively. The measurements follow the ISO 11146 standard, with a minimum of 10 different measurement planes in the z -range of ± 2 Rayleigh lengths around the focus. A minimum of 5 planes should lie within ± 1 Rayleigh length of the focus.

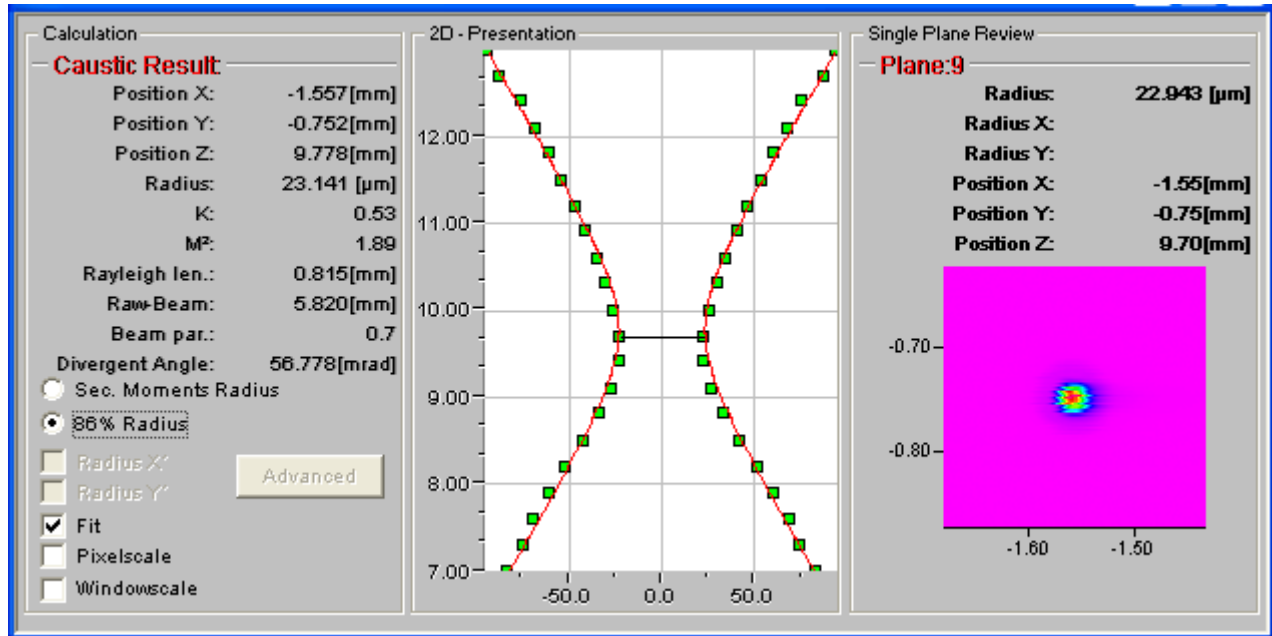


Fig. 7. The beam parameters for the single-mode fiber with $\omega_1 = 3.2 \mu\text{m}$ after passing an $f60/f205$ mm collimator/focusing optics. The caustic results are presented for the 86.5% radius ($1/e^2$). The BPP is determined to 0.66 and the $M^2 = 1.89$.

The beam parameters and the properties of a plane close to focus for the single-mode fiber with $\omega_1 = 3.2 \mu\text{m}$ is given in Fig. 7. The beam profile is slightly asymmetric, probably due to the imaging optics, but the astigmatism is low (0.04). The BPP is determined to 0.66, giving an $M^2 = 1.89$ at $\lambda = 1090 \text{ nm}$. The output from the QCS cable is specified to have a beam propagation ratio $M^2 = 1.07$.

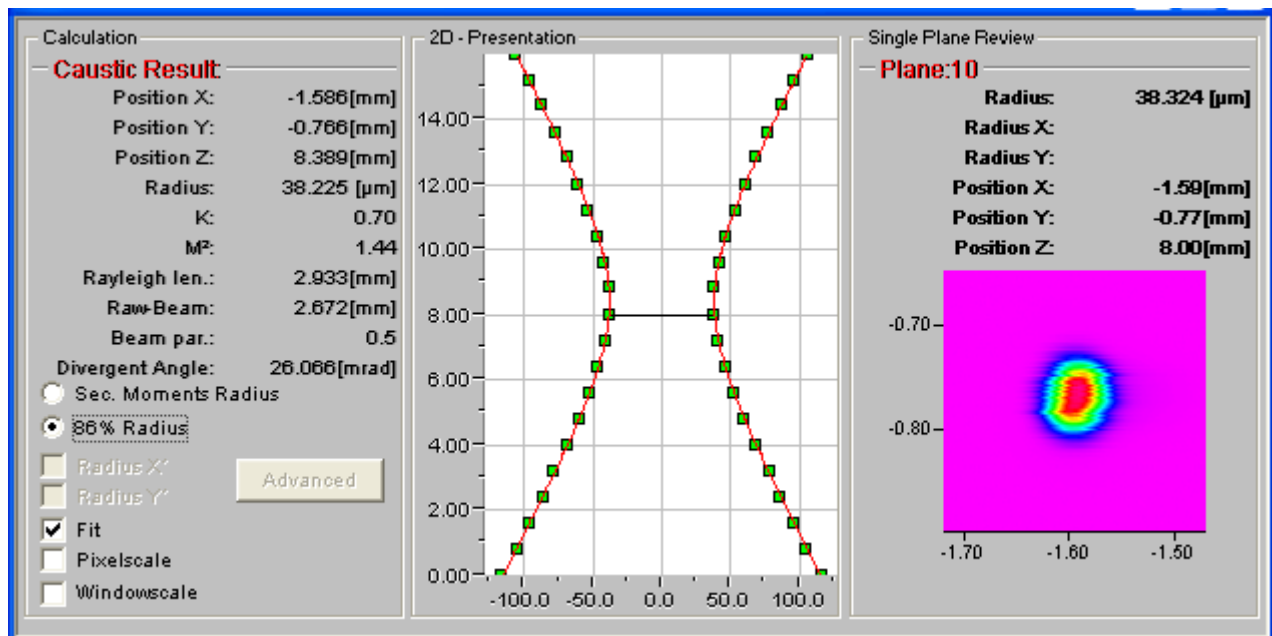


Fig. 8. The beam parameters for the large mode area fiber with $\omega_1 = 9 \mu\text{m}$ after passing an $f60/f205$ mm collimator/focusing optics. The caustic results are presented for the 86.5% radius ($1/e^2$). The BPP is determined to 0.50 and the $M^2 = 1.44$.

The beam parameters and the properties of a plane close to focus for the large mode area fiber with $\omega_1 = 9 \mu\text{m}$ is given in Fig. 8. Also here the beam profile is asymmetric, but the astigmatism is low (0.01). The BPP is determined to 0.50, giving an $M^2 = 1.44$ at $\lambda = 1090 \text{ nm}$.

5. CONCLUSIONS

In conclusion, free-space fundamental-mode fiber-to-fiber coupling have been investigated theoretically and experimentally regarding the sensitivity of the coupling efficiency due to misalignments of different types and expected power losses.

The theoretical study described the out-coupled field by a hyperbolic secant function, which is a much better approximation than the Gaussian function. The field around the image plane has been calculated numerically using the Fresnel-Kirchhoff integral transform, describing both the amplitude and phase distribution. The receiving fiber geometry has been described by its defocus, its radial displacement and its tilt, where the tilt is possible to neglect. The coupling efficiency has been calculated using overlap integrals between defocused field and the radially translated receiving fiber mode. The calculations for a symmetric case coupling a single-mode fiber with $\omega_1 = 3.2 \mu\text{m}$ using two $f = 24 \text{ mm}$ lenses into a single-mode fiber of the same kind shows small alignment tolerances, where a radial displacement of $3.7 \mu\text{m}$ reduces the coupling efficiency with 50 %. The defocus sensitivity is also significant. The asymmetric case coupling into a large mode area fiber with $\omega_1 = 9 \mu\text{m}$ using an $f = 50 \text{ mm}$ lens is much less sensitive to both radial misalignments and defocus, suggesting being the preferred solution.

The experimental results qualitatively confirms the numerical calculations, where using a 100 W fiber laser 88% coupling efficiency using the LMA fiber and 75 % coupling efficiency using the single-mode fiber has been measured. The beam profiles show an increase in beam propagation ration ($M^2 = 1.44$ and $M^2 = 1.89$ for the $\omega_1 = 9 \mu\text{m}$ and the $\omega_1 = 3.2 \mu\text{m}$ fibers, respectively). This increase is attributed to not perfectly coinciding optical axes for the collimating and focusing lenses at the exit side of the QB cable. Also, surface contamination of the $f60/f205$ lens system may increase the M^2 values.

Both the theoretical and experimental results suggest that free-space fundamental-mode fiber-to-fiber coupling is possible. In products for high-power (multi-kW) applications a coupling efficiency of better than 90% is necessary, where the excess heat has to be taken care of in the fiber connectors. Due to the small alignment tolerances thermally stable optics is required and possibly also a continuous auto-alignment of the receiving fiber.